Design and test of the plant-correcting reel for harvesting lodging garlic plants

Yuhua Li[1], Chao Li[1,2], Lupeng Liu[1], Kai Zhou[1], Jialin Hou[1*]

(1. *College of Mechanical and Electronic Engineering, Shandong Agricultural University, Tai'an 271018, Shandong, China*;
2. *College of Biosystems Engineering & Food Science, Zhejiang University, Hangzhou 310058, China*)

Abstract: Crops are prone to lodging with the decline of stem moisture and the intervention of other factors in the mature harvest period, such as garlic, which is difficult to harvest mechanically. To solve this problem, the plant-correcting reel for harvesting lodging garlic plants, bumped and deformed with plants many times to pull and lift them into a conveyor, was proposed in this study. This study analyzed the motion trajectory equation and key influencing factors of the reel and defined the lifting and plant-correcting stages as three processes of contact, stirring and release. For example, the contact deformation model and system energy equations were established in the contact process. Besides, in the stirring process, the garlic plant-correcting conditions were established through the dynamic simulation test analysis of garlic seedling trajectories and the deflection model of garlic stem was constructed. Furthermore, in the release process, the expressions of rubber bars rotation and garlic plant offset bending curvature were constructed and the optimal number and distribution form of bars were determined. Meanwhile, the mechanism and key operating parameters of the auxiliary lifting mechanism of the divider were established. Through the single-factor test, the influence of reel speed, forward speed and reel height on the success feeding rate was analyzed under different bars distribution forms; Through multi-factor experiments, the interaction contour map of various factors was constructed. When reel speed, forward speed and reel height were 3 rad/s, 3.5 m/s, and 540 mm, the feeding success rate was 98.73%. The optimization factors were tested and verified, which met the operational requirements of a high feeding success rate and low loss rate of garlic harvest. This study combines laboratory virtual as well as field experiments and analyzes of trajectory of bars, contact deformation and deflection model of garlic plant, and reel rotation and garlic plant offset bending curvature to solve the problem of garlic lodging mechanized harvest and yield reduction.

Keywords: feeding success rate, lodging, garlic, harvesting reel, plant model, field test
DOI: 10.25165/j.ijabe.20241701.7784

Citation: Li Y H, Li C, Liu L P, Zhou K, Hou J L. Design and test of the plant-correcting reel for harvesting lodging garlic plants. Int J Agric & Biol Eng, 2024; 17(1): 59–68.

1 Introduction

Garlic (*Allium sativum*) is an important cash crop with good edible and medicinal value[1,2]. China is the largest garlic producer and exporter in the world, and its annual export volume accounts for about 90% of the world's total trade volume[3,4]. When the garlic is mature, the moisture content of the stem and leaves will drop rapidly. Meanwhile, under the influence of natural and improper artificial conditions[5], garlic plants are prone to lodging, which is difficult to implement and popularize combined mechanized harvesting.

Garlic harvesting mechanization in developed countries started earlier, represented by medium and large garlic harvesters[6]. Large-segmented garlic harvesting equipment is mainly used in the United States and Canada. For example, the Garlic Windrower 2400 and Garlic Loader 2400 harvester developed by Top Air company can realize the excavation, picking, air separation, impurity removal and collection of garlic. Spain, France and other European countries mainly use medium-sized traction or backpack combined harvesters. The main representative garlic harvester manufacturers in Europe included JJ Broch company and ERME company in France, which is characterized by intelligence, miniaturization and serialization. Japan, South Korea and other Asian countries mainly use small self-propelled combined harvesters. The main representative garlic harvester manufacturer is YANMAR company in Japan, whose equipment is more intelligent, highly stable, has better fuel economy, and is more environmentally friendly. Since the 13th Five-Year Plan, with the support of national scientific research projects, the mechanization of garlic harvest in China has achieved rapid development, such as the 4S-6 and 4DS-45 combined garlic harvesters[7,8], which can realize the harvest of garlic within 180-220 mm row spacing.

Low-loss harvesting was a topic of high concern in the agricultural field, and lodging was an important factor in crop yield reduction and restricting mechanized operations. Many studies have worked toward solving this problem to decrease harvest loss. For example, Wu et al.[9] argued that Crop lodging has long been recognized as one of the severe constraints limiting production worldwide. Qing et al.[10] proposed that a harvesting reel with improved tine trajectory can push the reel into the crops, feed plants into the auger and release the reel, which would reduce crop loss rate. Hirai et al.[11] explored the relationships between the deflection and deflection force acting on a bunch of crop stalks in the

Received date: 2022-07-10 **Accepted date:** 2023-12-29
Biographies: Yuhua Li, PhD, Associate Professor, research interest: agricultural mechanization technology, Email: liyuhua@sdau.edu.cn; **Chao Li**, PhD, research interest: agricultural equipment design, Email: 12213019@zju.edu.cn; **Lupeng Liu**, MS, research interest: agricultural equipment design, Email: 812308272@qq.com; **Kai Zhou**, PhD, Associate Professor, research interest: agricultural equipment design, Email: zhoukai2017@sdau.edu.cn.
***Corresponding author: Jialin Hou**, PhD, Professor, research interest: agricultural equipment design. College of Mechanical and Electronic Engineering, Shandong Agricultural University, Tai'an 271018, Shandong, China. Tel: +86-13605388153, Email: jlhou@sdau.edu.cn.

gathering operations of a combine harvester reel and the quasi-static stalk bending crop model was established to evaluate the impact of the reel of the combine harvester on crops.

Previous research related to combined garlic harvesting has thoroughly investigated the digging shovel, conveyor and cutting knife in harvester parameters[12-14], which was based on the good verticality of garlic plants. However, garlic collapse is still common at maturity, which poses a major challenge to combine mechanized harvesting. Even worse, few studies on garlic harvest have focused on the mechanism and equipment of lifting and raising plants based on the lodging characteristics of garlic plants. In this study, a plant-correcting device was designed, and the motion trajectory equation of the reel, as well as the contact deformation and deflection model of the plant, were constructed to analyze the three stages of contact, stirring, and release. Through the repeated bumping and deformation of flexible rubber bars and plants, lodging garlic plants were pulled and lifted onto the conveyor, thereby improving the feeding success rate.

2 Materials and methods

2.1 Characteristics of garlic plants

Different from wheat, rice, rape, and soybean, garlic (*Allium sativum* L.) is a typical vegetable and herb of the genus Allium in the family Liliaceae[15]. According to its morphology and purpose, it can be divided into two types, namely bolt garlic and non-bolt garlic, among which, non-bolt garlic maturing in different periods is a widely cultivated variety currently. Although bolt garlic is not widely planted, bolt harvesting is a very necessary work for the enlargement of the bulb and the improvement of yield. In general, garlic average height is greater than 500 mm, which there are more than 5 leaves around the stem, its geometry is shown in Figure 1a.

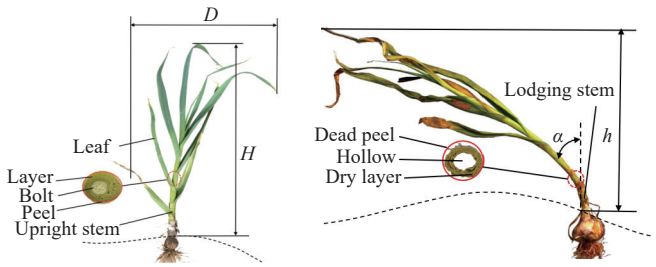

a. Upright garlic plant b. Lodging garlic plants

Figure 1 Characteristics of garlic plant

Garlic stems are composed of peels, layers and bolts. In the first two weeks of garlic ripening, garlic bolts are usually removed from the plant, which the soft layers are the main component of the stem. Especially, when garlic reach maturity, the moisture content of stems and leaves will gradually decrease, which catalyze inclined and lodging garlic plant[16-18]. After the garlic plant lodging, its effective height from the ground will reduced, as exhibited in Figure 1b. Garlic plants are prone to lodging in the mature period, which makes them very difficult to harvest mechanically. Consequently, the particularity of Garlic plants should be considered to determine the optimal design.

2.2 Structure and working principle

During the harvest, the main function of the plant-correcting device was stirring the lodging garlic plants and guiding them to convey, which can improve harvesting efficiency of lodging plants. The plant-correcting device was loaded at the front side of the conveyor and mainly consisted of a rotating shaft, universal joints, bevel gears, bearings, rigid brackets, rubber bars, a divider, a depth limiting wheel, etc., as shown in Figure 2.

Horizontal displacement of rubber bars in the opposite direction of the harvester is necessary to achieve upward movement of garlic stems, which requires the circumferential speed of rubber bars in the reel to be greater than the harvester's forward speed. The theoretical stage of plant-correcting is interpreted via three processes including the stage of contact, stir, and release[10], as shown in Figure 3.

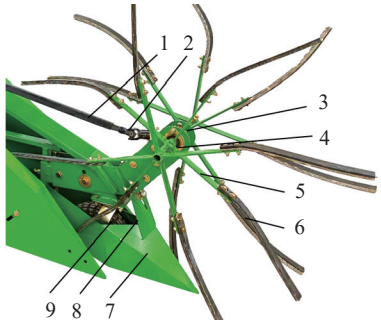

1. Rotating shaft 2. Universal joint 3. Bevel gear 4. Bearing 5. Rigid frame 6. Rubber bar 7. Divider 8. Angle adjusting device 9. Depth limiting wheel

Figure 2 Structure diagram of plant-correcting device

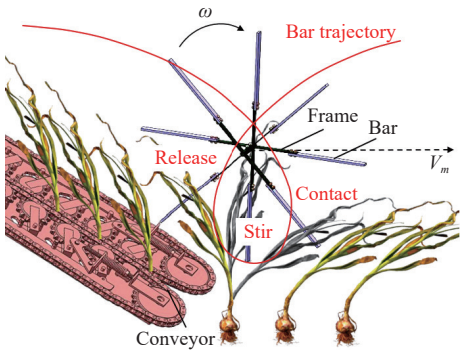

Figure 3 Plant-correcting process of the reel

In the process of contact, the rubber bar collided with the garlic plant and affected its movement. Moreover, the contact position where the garlic plant is moved by the rubber bar is the leaves on both sides of the stem or the curved stem. Therefore, the ground clearance of the reel is an effective working factor to be considered. When the rubber bar contacts the garlic plant, the actual horizontal trajectory of the rubber rod is opposite to the forward direction of the harvester, which means that the stirring process comes. In this process, the lodging garlic plants are lifted and the maximum ground clearance of garlic seedlings is higher. The release process is the final process when the bar pushes the plants to the conveyor and stays away from them to prevent them from being tangled around the reel. In this stage, the horizontal movement trajectory of the bars is the same as the forward direction of the harvester.

2.3 Plant-correcting process and main parameter design

The main structural parameters of plant-correcting device include the diameter and installation height of the reel, and the evaluation index is the lifting efficiency, as shown in Figure 4. The coordinate system is established in the center of seedling correcting device, the forward direction is set to the x-axis direction, and the y-axis is vertical to the forward direction. (x_1, y_1) is the initial coordinate position of the first rubber bar edge, (x_2, y_2) is the position of the second rubber rod edge after rotation and (x_n, y_n) is the position of the nth rubber rod edge after rotation.

The trajectory equation of rubber bar was[8]:

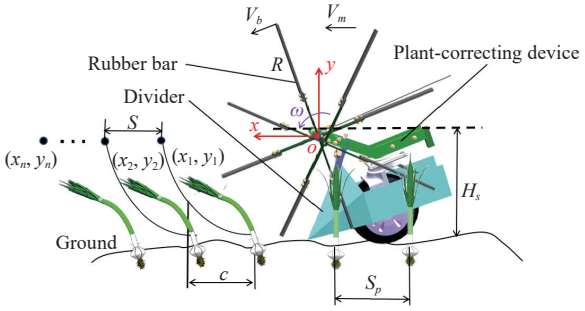

Note: c is the effective threshing distance for half revolution, mm; h_s is the shortest distance between rubber bar edge and ground, mm; H_s is the distance from the center of rotation to the edge of the bar, mm; V_b is the bar edge velocity, mm/s; R is the length of the rubber bar, mm; S_p is the advance distance of combined garlic harvester when the rubber bar rotates 90°, mm; ω is the angular velocity of seedling correcting device, rad/s.

Figure 4 Reel movement and lifting process

$$\begin{cases} x = v_m t + R\cos\omega t \\ y = (H_s + h_s) - R\sin\omega t \end{cases} \tag{1}$$

When the rubber bar rotates once, the combined garlic harvester moved forward by:

$$s = \frac{8\pi}{z\omega} v_m \le S_p \tag{2}$$

The effective threshing distance for one revolution can be expressed as:

$$C = 2c = \frac{V_m R}{V_b}\left[\arcsin\frac{V_m}{V_b} + \sqrt{\left(\frac{V_b}{V_m}\right)^2 - 1} - \frac{\pi}{2}\right] \tag{3}$$

To achieve the ideal plant-correcting effect of the reel and reduce the damage of garlic seedling before clamping, it is necessary to establish the speed ratio λ between the machine forward speed and the bar edge velocity, and effect index of seedling correction device η:

$$\eta = \frac{z v_m}{4\pi R}[\arcsin(\lambda^{-1}) + 2\sqrt{\lambda^2 - 1} - \pi] \tag{4}$$

where, λ represents the reel speed ratio, which denotes the speed ratio between the forward speed of the machine and the velocity of the bar edge, thereby influencing the trajectories of the rubber bars; η *is* the effect index of seedling correction device, which represents the level of garlic seedlings corrected by rubber rod. It can be obtained by Equation (4) that the effect index of seedling correction device η was affected by the speed ratio λ. To avoid the damage of garlic straw, the speed ratio value should not be too large.

2.3.1 The process of contact

The reel component consists of flexible rubber bars installed on a rigid frame, which causes continuous contact and collisions between the rubber bars and garlic plants. One side of the rubber bars is fixed, while the other side is free. To describe the deformation of the rubber bar lifting garlic plants, the Euler-Bernoulli beam theory can be cited to define the rubber bar as a flexible beam[19]. As shown in Figure 5, P and Q are the points where the rubber bar is about to contact the garlic plant. The coordinate system XOY is established at the connection point between the rubber bar and the rigid frame. When the contact process came, point P in the flexible rubber bar coincided with point Q in the garlic plant, and point P began to deform to P' where a short-duration slipping motion also occurred.

The deformation displacement can be expressed as:

$$\begin{cases} u_x = -\frac{1}{2} B^{\mathrm{T}}(t) Z(x_p) B(t) \\ u_y = \varphi_y(x_p) B(t) \end{cases} \tag{5}$$

where, $B(t)$ denotes the time-varying amplitude of mode; $Z(x_p)$ denotes the coupling deformation matrix; $\varphi_y(x_p)$ denotes the transverse mode array of flexible rubber bar. The system kinetic energy T and elastic potential energy V by the contact deformation of the rubber bar are as:

$$T = \frac{1}{2}\int_0^L \rho A(\dot{h}_M^{\mathrm{T}} \dot{h}_M)\mathrm{d}x \tag{6}$$

$$V = \frac{1}{2}\int_0^L EA\left(\frac{\partial u_x}{\partial x}\right)^2 \mathrm{d}x + \frac{1}{2}\int_0^L EI\left(\frac{\partial^2 u_y}{\partial x^2}\right)^2 \mathrm{d}x \tag{7}$$

where, h_m is a random point in the coordinate system XOY; ρ is the quality parameter of rubber gear; A is the cross-sectional area; E is the young's modulus; I is the sectional moment of inertia.

Kuwabara and Kono[20] considered a collisional event by a Hertzian elastic contact with internal friction as the energy dissipation source. The viscoelastic contact force model is expressed as:

$$F_c = \frac{5}{4}(u_x^2 + u_y^2)^{3/4} + \gamma'\left(u_x^2 + u_y^2\right)^{1/4} \frac{\mathrm{d}\left(u_x^2 + u_y^2\right)^{1/2}}{\mathrm{d}t} \tag{8}$$

where, F_c is the force caused by the collision between garlic plants and rubber bars; γ is the dissipation factor, which is proportional to the contact velocity and the square root of the particle deformation; t is the normalized contact time.

Due to the mutual deformation between garlic plants and rubber bars, it can be considered that the deformation of garlic plants was equivalent to the deformation of rubber bars, denoted by μ. After normalizing Equation (8) by the contact duration and the maximum deformation, the deformation contact model of garlic plants can be expressed as:

$$\frac{5}{4}\mu^{3/2} + \gamma\mu^{1/2}\frac{\mathrm{d}\mu}{\mathrm{d}t} + \frac{\mathrm{d}^2\mu}{\mathrm{d}^2 t} = 0 \tag{9}$$

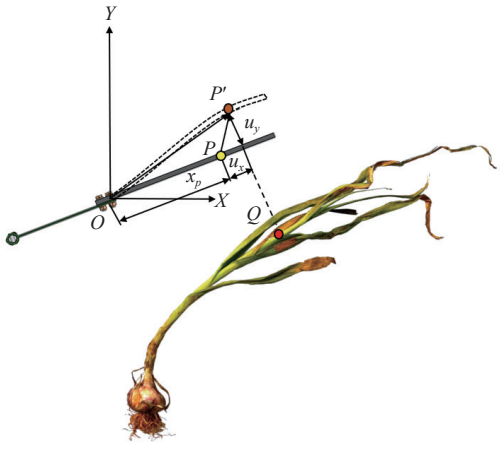

Figure 5 Contact between rubber bar and garlic plant

2.3.2 The process of stir

In the stirring process of the reel, when the linear rotation speed of the rubber bar is less than or equal to the forward speed, $\lambda \le 1$, the moving track line of the rubber bar has no intersection, which means that there is no horizontal backward speed of the rubber bar. So the lifting function of the garlic plant cannot be realized; When the linear rotation speed of the reel is greater than the forward speed, $\lambda > 1$, there is a closed-loop in the trajectory of the bar, when

the reel can continuously push garlic plants to the conveyor, as shown in Figure 6.

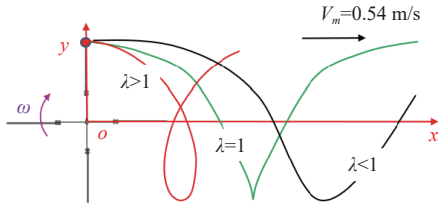

Figure 6 Trajectories of reel under different speed ratio

To realize the function of correcting garlic seedlings and determine the appropriate speed ratio, an ADAMS kinematic simulation model is needed, as shown in Figure 7. The model of the plant-correcting reel was established in SolidWorks software, then simplified and imported into ADAMS software, which is defined as a rigid body. The material parameters such as the density, Young's modulus and Poisson's ratio of the rubber gear are set 1000 kg/m^3, 7.84×10^6 Pa and 0.47. In ANSYS software Solid186 to construct garlic plant model and mat orthogonal anisotropy is selected as the material type[8]. The material parameters of garlic plant such as density, Young's modulus and Poisson's ratio are set to 438 kg/m^3, 1.1×10^{-10} Pa and 0.33.

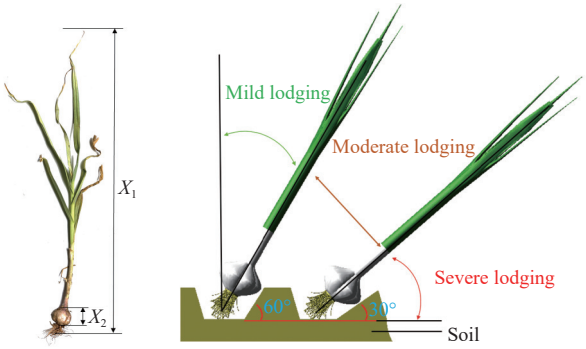

Figure 7 Model diagram of garlic plant

Because of the moisture content decreased of garlic stem in the mature stage, the inclination of garlic stem is varying. A definition is given: when the angle between garlic stem and the ground is more than 60°, it is mild lodging; when the angle is between 30° and 60°, it is moderate lodging; when the angle is less than 30°, it is severe lodging[21,22].

In order to find the appropriate ratio of reel speed to forward speed, a large number of tests had been done[8]. As shown in Figure 8, under the premise of forward speed of 0.54 m/s, when the reel speed is less than 2.6 rad/s, although the value of λ is greater than 1, the garlic plant still cannot be lifted at this time. Due to the fact that the garlic plants are unable to reach the purpose of vertical posture at all, when the reel speed is between 2.6 rad/s and 2.9 rad/s, the garlic plants can reach the purpose of lifting the garlic plant, but it is not straightened in sequence. When the reel speed is greater than 2.9 rad/s, garlic plants are lifted in turn to the promising posture, which the value of λ is greater than 2.7.

The garlic plant experienced a force from the rubber bar F, and was additionally impacted by its own gravitational force G, as well as the friction, F_m, that arose due to relative motion between the rubber bar and the garlic plant[23]. As a result, the garlic plant rotated in the opposite direction to the forward motion of the harvester, leading to a bending moment M, as shown in Figure 9. The equilibrium equation was derived as follows:

$$\begin{cases} F\sin\gamma_m + G - \mu_f F\cos\gamma_m = 0 \\ h_{ym}(F\cos\gamma_m + \mu_f F\sin\gamma_m) + M = 0 \end{cases} \tag{10}$$

where, γ_m denotes angle between the external force F and horizon, which could also be defined as the angle between the garlic plant and the vertical line; μ_f is the friction coefficient between garlic plants and rubber bars; h_{ym} denotes the vertical height of the contact point between the rubber bars and the garlic plant. Based on the elementary theory of elastic bending theory[24], at the point of the deflected cantilever, which could be described as:

$$\cos(\gamma_m - \gamma) = \frac{F}{EI}(L_m - L)\mathrm{d}L \tag{11}$$

where, EI denotes flexural stiffness, N·m^2; F denotes external force on deflecting of garlic plant. L_m denotes the moment from external force F to deflection center, m. It is assumed that EI varied with L and may be represented in the form of a Taylor-McLaurin polynomial[25] as follows:

$$\frac{1}{EI} = \frac{1}{E_0 I_0}\left(1 + \sum_{i=1}^{k} A_i L^i\right) \tag{12}$$

where, E_0I_0 corresponded to the base flexural stiffness of the cantilever, N·m^2; A_i was a parameter related to the mechanical properties of different parts of garlic stems, and (k+1) is the number of terms in the Taylor-McLaurin polynomial. The deflection model of garlic plant could be obtained by combining Equations (11) and (12):

$$\sin\gamma_m = \frac{1 + \sum_{i=1}^{k}\left[\left[\frac{2}{(i+1)(i+2)}\right]A_i L_m^i\right]}{2E_0 I_0} FL_m^2 \tag{13}$$

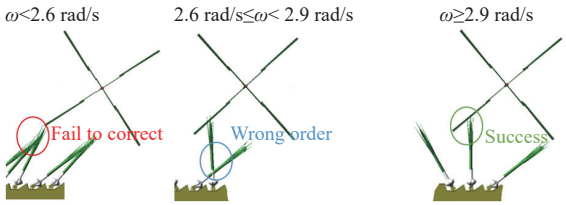

Figure 8 Garlic plants correction simulation experiment

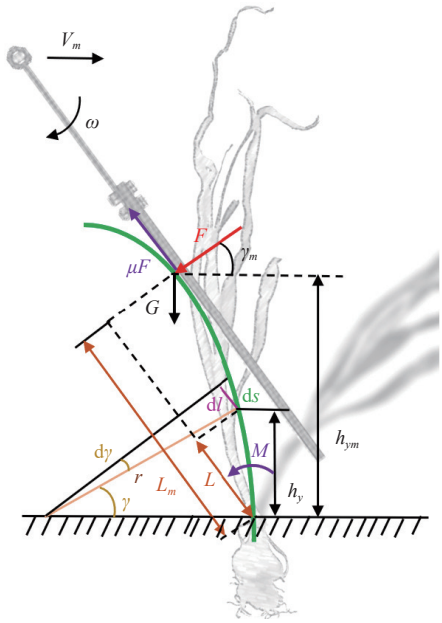

Figure 9 Transformed model of a deflected stem

To simplify the model, new variable B_i was introduced:

$$B_i = \sum_{i=1}^{k} \left[\left[\frac{2}{(i+1)(i+2)} \right] A_i L_m^i \right] \tag{14}$$

B_0 is a constant coefficient and B_0=1 then the deflection model of garlic plant could be simplified as follows:

$$\sin\gamma_m = \left[\sum_{i=1}^{k} B_i \right] \frac{FL_m^2}{2E_0 I_0} \tag{15}$$

The new balance equation could be obtained by combining Equations (1), (10) and (15):

$$\sum_{i=1}^{k} B_i \frac{F^2((H_s+h_s)-R\sin\omega t)^2}{2E_0 I_0} + G - \frac{\mu_f F \sqrt{\left(4E_0^2 I_0^2 - F^2((H_s+h_s)-R\sin\omega t)^4 \left(\sum_{i=1}^{k} B_i\right)^2\right)}}{2E_0 I_0} = 0 \tag{16}$$

According to Equation (16), it is observed that the stress distribution and deformation of the garlic plant during the harvesting process are closely related to the height and speed of the reel, the mechanical properties of the garlic stem, the elastic model, and the height of the cross-sectional moment of inertia.

2.3.3 The process of release

At the end of the stir process, it is necessary to evaluate the plant-correcting effect of the rubber bars and the crop deflection model applied to the determination of plant-correcting reel stagger, as shown in Figure 10.

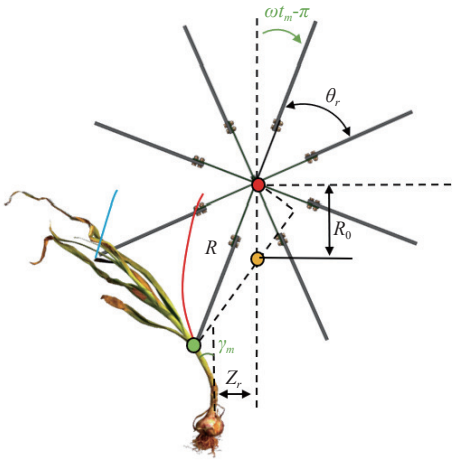

Figure 10 Influence of rubber bars' kinematic parameters

When the velocity of ascending bars became tangential to the curvature of deflected stems, the process of stir had reached the end. The angle at which the rubber bar moved from the top and rotated tangent to the deflected stem can be expressed as:

$$\omega t_m = \cos^{-1}\left(\frac{R_0}{R}\cos\gamma_m\right) + \pi + \gamma_m \tag{17}$$

where, ω denotes plant-correcting reel rotation angular speed, rad/s; t_m denotes the length of time that the rubber bar moves from the top and rotates tangent to the deflected stem, s; R denotes rotation radius of the plant-correcting reel, m; R_0 denotes labeled vertical distance, being equal to the reel advance per radian of rotation, m.

To achieve the best correcting effect, when the leading rubber bars are far away from deflected stems, the lagging bars should be in such a position as to contact the stems. However, during the actual operation, some garlic stems may be sandwiched between those deflected by the leading rubber bar and those deflected by the lagging rubber bar. To obtain the number of rubber bars, the motion interference between multiple garlic plants is not considered here. Therefore:

$$\theta_r = \omega t_m - \pi - \sin^{-1}\left(\frac{Z_r}{R}\right) \tag{18}$$

$$n = \frac{2\pi}{\theta_r} \tag{19}$$

where, n denotes the number of rubber bars; Z_r denotes plant-correcting reel stagger, mm; θ_r denotes the angle between adjacent rubber bars, which could be obtained:

$$n = \frac{2\pi}{\cos^{-1}\left(\frac{R_0}{R}\cos\gamma_m\right) + \gamma_m - \sin^{-1}\left(\frac{Z_r}{R}\right)} \tag{20}$$

It could be obtained by substituting the actual value into Equation (20) that the number of rubber bar was 8, and garlic stems could be effectively transferred to the conveyor. According to the arrangement form of rubber bars, it could be divided into interlaced distribution form, centralized distribution form, and similar distribution form, as shown in Figure 11.

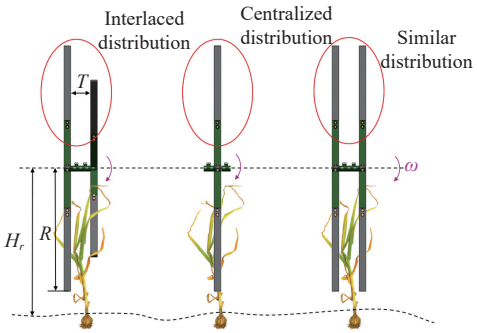

Figure 11 Three different installation patterns of rubber bars

Among them, if the rubber bars are interlaced, the rubber bars on one side could fulfill the function of harvesting garlic, while the bars on the other side could prevent the garlic plant from leaning and deviating. If the rubber bars are centralized, it would increase the threshing intensity, which is conducive to continuous harvest feeding. However, at the same time, the harvester should have a good row-harvesting capacity. On the other hand, if the rubber bars are similarly distributed, it would enhance the ability of fallen garlic plants to be righted in all directions, potentially causing the garlic stalks to wind around the central area of rotation. Three types of distribution forms of rubber bars would test subsequently, to optimize the layout of the bars and improve the feeding rate.

There is no standardized row spacing for garlic planting across different regions of China. However, row spacing typically ranged between 180-220 mm[6]. The effectiveness of harvesting is influenced by both the horizontal arrangement of rubber bars on the harvesting wheel and the alignment between garlic planting techniques and machine operation. To accommodate diverse agronomic requirements, an adjustable reel spacing is designed. The installation distance T between the left and right rubber bars is the critical parameter for achieving optimal horizontal reel distribution. Based on Figure 12, the horizontal distribution and planting configuration of the reel, the T value can be determined as follows:

$$\sigma + 2\mu + \lambda' \le T \le D \tag{21}$$

By Equation (21), the optimal installation distance between the left and right rubber bars T was found to be within the range of 154-220 mm. After conducting multiple tests, we determined that the best calibration results were achieved at an installation distance of 180 mm between the left and right rubber bars.

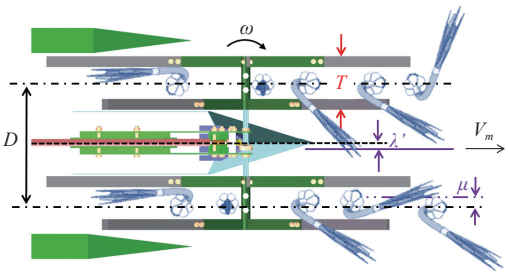

Figure 12 Horizontal arrangement of the reels

To realize the functions of stable operation and high-efficiency garlic plant lifting, the structure of the transmission system needed to be innovatively designed[26-28]. The divider is located in front of the garlic combine harvester and rigidly connected with the underframe with bolts, which could pick up and straighten the branches of lodging garlic plants as the harvester moves forward. Then, the height-adjustable plant-correcting device pulled the disorderly garlic plants into the conveyor. The key components of the plant-correcting device were mainly the central rotating spline shaft and the frame rigidly connected with the shaft. The end of the rubber bars connected with the frame support with bolts, which could realize the function of the plant straightens with the rotation of the central spline shaft.

The power of the plant-correcting device came from the gasoline engine. The speed of the engine power output shaft is 3600 r/min. The reducer gear box with a speed ratio of 0.05 is connected with the engine to realize the transmission effect of speed reduction and torque increase. This box output power shaft is connected with the transmission assembly to realize the speed ratio change from 0.46 to 2.15, so as to facilitate the adjustment of test parameters, as shown in Figure 13. The output shaft of the variable speed transmission assembly transmitted power to the long rotating shaft transmission system by the chain, the bevel gear and the belt. Because of the structural design of the harvester body, the power is transmitted to the harvester through the long-distance rotating shaft. The universal joints are used to connect the power transmission of the rotating shaft, while the bevel gears divide the power of the rotating shaft into spline shafts on both sides and the plant-correcting device rigidly connected with the shaft, and the output input speed ratio of the bevel gear set was 0.33. Finally, the adjustable speed of the plant-correcting bar is 28-130 r/min in the garlic plants lifting test.

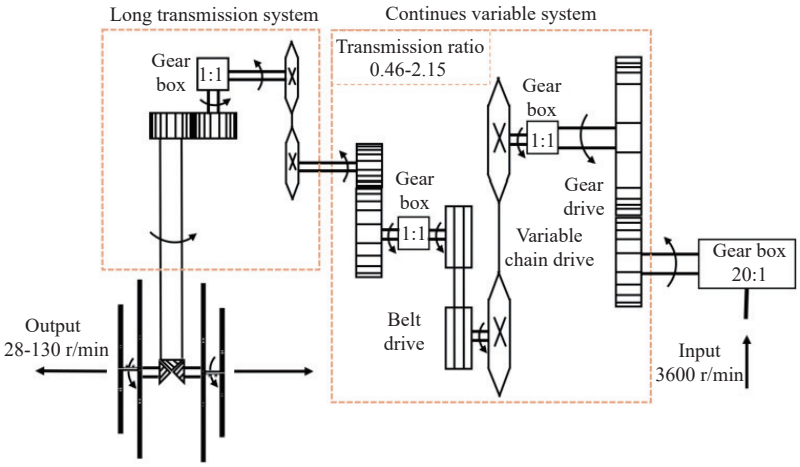

Figure 13 Power transmission route map of plant-correcting device

2.4 Mechanism and parameter design of divider

The lodging direction of garlic plants is irregular, so lodging angle and side angle[22] are introduced to describe the lodging level of garlic. The lodging angle α denotes to the angle between the garlic plant and the vertical line, and side angle β denotes to the angle between the garlic plant and the forward direction of the harvester.

In the harvesting process, the function of the divider is to branch and lift the lodging garlic plants to reduce the harvest loss. To be more specific, the distance from the ground to the contact point between the divider and plants became larger with the lodging plants being lifted and the lodging angle and side angle decreased gradually, as shown in Figure 14a. The research shows that the cone corner angle of the divider and the height from the top of the divider to the ground are the most important factors to determine the performance of the divider[29]. As shown in Figure 14b, the stress of garlic plant was analyzed, and we could get:

$$\begin{cases} F' \cdot \sin\dfrac{\theta_0}{2} = N \\ F' \cdot \cos\dfrac{\theta_0}{2} \ge f \\ f = \mu N \end{cases} \tag{22}$$

The static friction coefficient between garlic plant and metal was obtained from relevant literature, μ=0.2-0.6, so it could be obtained that the value space of the cone angle of the divider was [30°, 60°][30]. Combined with the agronomic requirements of plants and the installation width of depth limiting wheel, the cone angle θ_0 of divider was finally designed to be 40°.

When the tip of the divider is closer to the ground, it is more conducive to effectively supporting the grain. To harvest garlic that has deflected to the ground, the tip of the divider should be positioned where the soil is just covering it. However, excessive burial may increase travel resistance. Taking cues from the Bentleg-type machine, the soil penetration angle η is designed

to be 20° to facilitate soil flow and reduce forward resistance. In this context, soil disturbance parameters such as critical depth, furrow depth, ridge height, and furrow width are described in Figure 12b.

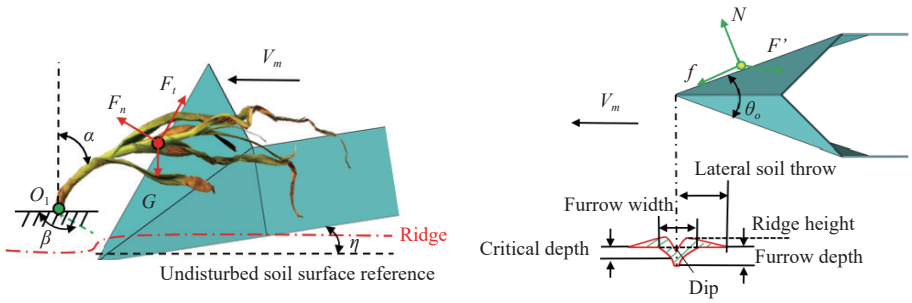

a. Effect on deflectedgarlic plant b. Effect on soil

Figure 14 Schematic diagram of working principle of divider

3 Test and result analysis

3.1 Test conditions and methods

To determine the best working parameters of the plant-correcting device of the garlic combine harvester, the virtual simulation and multi factor outdoor tests were carried out in the Intelligent Equipment Virtual Simulation Laboratory of Shandong Agricultural University on April 20, 2021, and in the An Shun agricultural planting professional cooperative of Henan province on April 23, 2021. In the early 10 d of April, the early maturing garlic in An Shun Agricultural Planting Professional Cooperative ripened faster after bolting, and the stem was also prone to lodging, so it is a more suitable place for testing. Before the test, the divider was put between the two rows of garlic plants in the test field. The rubber bars installed on the harvester were distributed on both sides of the garlic plant. As the garlic harvester moves forward, the divider divided the garlic plants into two rows and lifted the lodging garlic plants in the opposite direction of advance. The plant-correcting device pulled the lodging garlic plants in front of the machine and others corrected by the divider into the conveyor to realize the smooth clamping and harvesting of garlic plants.

3.2 Simulation and bars trajectory analysis

When the reel rotated at 2.9 rad/s, by setting the harvester forward speed to 0.45 m/s, with a reel speed ratio λ=2.7, from Figure 15a it could be seen that the motion trajectory of the rubber bars had an obvious return and had a certain distance gap in the forward direction, which could realize the pulling and lifting of garlic plants. In addition, there was a spatial displacement relationship between the motion trajectories of the rubber bars on different sides, including the horizontal distance in the forward direction and the vertical distance in the direction of the rotation spline shaft. The shape was similar to the motion trajectories of the bars on the same side, meanwhile, the bars on the other side could pull and push the garlic plants again, which could adapt to the garlic plants lodging in disorder and improve the success rate of the garlic plants in pulling into the conveyor.

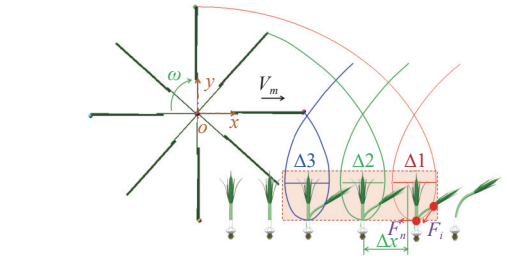

a. Bars trajectory of plant-correcting device

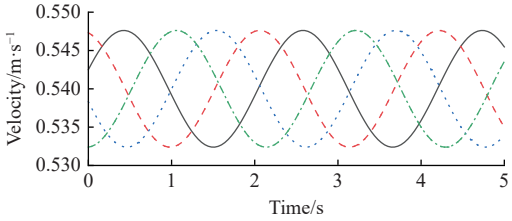

b. Velocity curve of bars of plant-correcting device

Figure 15 The bars trajectory and velocity under the reel speed ratio (λ) of 2.7

In Figure 15b, the vertical speed of the rubber bars presented a stable fluctuation value, reflecting the stable plant-correcting process of contact, stir and release, in which maximum and minimum values appeared after release and before entering the plant, to achieve the continuous and stable lifting and stirring in the stirring stage.

3.3 Test factors and index selection

Reel rotation speed, harvester forward speed and reel vertical height were selected as the test factors[31,32], and the feeding success rate of the reel is used as the evaluation index of plant-correcting. On the basis of the influence of the dividing and supporting of the divider, if the plant-correcting reel failed to pull the garlic plants into the conveyor, or failed to meet the clamping and positioning requirements, it was a failure of plant-correcting. The positioning requirement of the garlic bulb was that there is a vertical clamping error range within 100 mm. Therefore, under the influence of the plant-correcting reel, if the clamping position of the garlic plants in the section of the stem was within 100-200 mm above the garlic bulb, it was a success of plant-correcting. However, in the actual process of plant-correcting, the clamping height of the garlic stem at the front side of the conveyor cannot be monitored in real time. Therefore, the following definition was made, if the length of the garlic bulb that falls into the garlic barn after cutting is within 15-25 mm (did not affect the transportation, sale and storage of garlic), it was a success of plant-correcting. The calculation result of the feeding success rate of the reel could be equal to the ratio of garlic bulb mass with qualified length in the garlic barn to the total mass of garlic bulb in the garlic barn and picked up manually on the ground.

3.4 Test scheme

The rotation speed of plant-correcting device and the forward speed of the harvester determined the motion trajectory of the rubber bars[33]. According to above theoretical calculation and motion simulation, the speed ratio of the harvester was determined,

so the value range of the reel rotation speed was 2.5-3.5 rad/s. Based on the actual operation efficiency requirements of garlic harvest and the design of the transmission scheme of the harvester, the value range of the forward speed of the harvester was 0.3-0.6 m/s. The maximum reel vertical height should not be higher than the sum of the gravity center of the garlic plant and the radius of the reel, and the rubber bars should not touch the ground under the minimum installation height of the reel, so the value range of the installation height of the reel is 500-600 mm. To study the influence of various factors on the test, using the response surface method to build a multi-factor evaluation model, the scheme of the test index influencing factors is listed in Table 1.

Table 1 Actual value and code of the variable

Levels	Reel Speed x_1/rad·s^{-1}	Forward speed x_2/m·s^{-1}	Reel height x_3/mm
–1	2.5	0.30	500
0	3.0	0.45	550
1	3.5	0.60	600

In order to study the influence of various factors on the feeding success rate, the garlic harvester retained the devices such as the plant-correcting mechanism, conveyor and straw cutting mechanism. The forward distance of the garlic harvester is 10 m and each test was repeated 5 times. The test results are taken as the average value and the process of the test is shown in Figure 16.

Figure 16 Field test of plant-correcting device

3.5 Test results and parameter optimization

In the rotation speed test of the reel, the forward speed of the garlic harvester and the installation height of the reel were 0.45 m/s and 550 mm respectively. The reels with interlaced, centralized and similar rubber bars distribution were tested at different rotation speeds of 2.5 rad/s, 3.0 rad/s, and 3.5 rad/s respectively, which results are shown in Figure 17a. As the rotation speed of the reel increased, the feeding success rate of different types of reels increased significantly. This was because the rotation speed of the reel increased, and the contact frequency between the rubber bars and the lodging garlic plant increased, which was conducive to pulling and lifting the lodging garlic plants. However, too fast the rotation speed of the reel would cause damage to the garlic plant and increase the interference of other rubber bars, making it difficult to separate the garlic plant from the reel. In the harvester forward speed test, the rotation speed and installation height of the reel were 3.0 rad/s and 550 mm respectively. The reels with interlaced, centralized and similar rubber bars distribution were tested at different harvester forward speeds of 0.30 m/s, 0.45 m/s, and 0.60 m/s respectively, which results are shown in Figure 17b. As the harvester's forward speed increased, the feeding success rate of different types of reel decreased significantly. This was because the harvester's forward speed increased, and the return stroke of the rubber bar was shortened, which affected the garlic plant relatively reduced. In the installation height test of the reel, the forward speed of the harvester and the rotation speed of the reel are 0.45 m/s and 3.0 rad/s respectively. The reels with interlaced, centralized and similar rubber bars distribution were tested at different installation heights of 500 mm, 550 mm, and 600 mm respectively, which results are shown in Figure 17c. As the installation height of the reel increased, the feeding success rate of different types of reel decreased. This was because the distance between the rubber bars and the ground increased, and the lifting efficiency of lodging garlic plants was poor, which effect on the garlic plant was relatively reduced. The contact point of rubber bars could not be higher than the gravity center of garlic plants, but it could not be too low, otherwise, it would increase the power consumption of lifting plants.

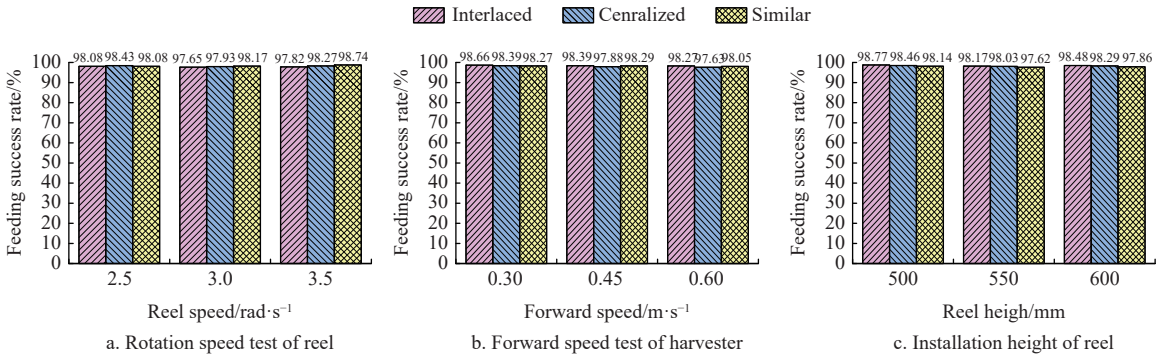

a. Rotation speed test of reel b. Forward speed test of harvester c. Installation height of reel

Figure 17 Results of single factor tests

On the other hand, the feeding success rate of the reels with interlaced was higher than that of others under the three working conditions. That meant the reels with interlaced were more suitable for pulling and lifting lodging garlic seedlings. Therefore, under the interlaced distribution of rubber bars, the rotation speed of the reel, to reduce the harvest loss, it is necessary to establish a more appropriate rotation speed of the reel, the forward speed of the harvester and the installation height of the reel.

According to the field operation requirements of the garlic combine harvester, taking the feeding success rate Y_1 as the response value, the reel speed X_1, forward speed X_2 and reel height X_3 were tested. The multi factor test scheme and results are listed in Table 2.

The data in the table were fitted by multiple linear regression and analyzed by variance with Design-Expert software. The results are listed in Table 3.

According to the data analysis of feeding success rate Y_1 of the reel, the coefficients of X_1, X_2, X_3, X_1X_2, X_1X_3, X_2X_3, X_1^2, X_3^2 were

significant at the level of $p<0.01$, and the rest are not significant. The model $p<0.01$ showed that the regression model of feeding success rate Y_1 as the response function was significant, the mismatch term $p>0.05$, and the mismatch was not significant. The regression model equation had a high degree of fitting, and the regression equation was:

$$Y_1 = 98.46 + 0.23X_1 - 0.10X_2 - 0.11X_3 + 0.49X_1X_2 + 0.71X_1X_3 + 0.35X_2X_3 - 0.61X_1^2 - 0.54X_3^2 \quad (23)$$

Table 2 Test scheme and results

No.	Reel speed X_1	Forward speed X_2	Reel height X_3	Feeding success rate Y_1/%
1	0	1	–1	97.62
2	1	0	–1	96.95
3	0	0	0	98.43
4	0	0	0	98.57
5	–1	0	1	96.25
6	0	–1	–1	98.47
7	0	0	0	98.53
8	0	1	1	98.06
9	1	–1	0	97.68
10	–1	–1	0	98.27
11	1	0	1	98.18
12	1	1	0	98.42
13	–1	0	–1	97.87
14	0	0	0	98.42
15	0	–1	1	97.52
16	0	0	0	98.37
17	–1	1	0	97.03

Note: X_1, X_2, and X_3 are the level values of experimental factors.

Table 3 Test scheme and results

Item	Sources	Sum of squares	Mean square	F	p
Y_1	Model	7.06	0.78	139.60	<0.0001
	x_1	0.41	0.41	72.86	<0.0001
	x_2	0.082	0.082	14.59	0.0065
	x_3	0.10	0.10	18.01	0.0038
	x_1x_2	0.98	0.98	174.37	<0.0001
	x_1x_3	2.03	2.03	361.28	<0.0001
	x_2x_3	0.48	0.48	85.94	<0.0001
	x_1^2	1.56	1.56	278.29	<0.0001
	x_2^2	0.000 085	0.000 085	0.015	0.9054
	x_3^2	1.24	1.24	220.06	<0.0001
	Residual	0.039	0.005 621		
	Misstated item	0.012	0.003 942	0.57	0.6624
	Pure error	0.028	0.006 880		
	All items	7.10			

Note: $p<0.01$ (highly significant, **); $p<0.05$ (significant, *)

The Design-Expert software was used to analyze the test data and the Origin software was used to generate a two-dimensional interaction contour map to determine the influence of various factors on the feeding success rate Y_1, as shown in Figure 16.

Figure 16 shows the influence results of contour lines between various factors. Figure 16a shows the influence of factors such as reel speed X_1 and forward speed X_2 on the feeding success rate of reel Y_1. From the contour map, it could be seen that when reel height was 550 mm, with the increase of forward speed, to get a better response value of feeding success rate, the optimal value of reel speed was also increasing correspondingly, which had a significant interaction between reel speed and forward speed. Figure 16b shows the influence of factors such as reel speed X_1 and reel height X_3 on the feeding success rate of reel Y_1. From the contour map, it can be seen that when the forward speed was 0.45 m/s, the installation height of the reel was 525-575 mm, and which response value was better. When the reel speed increased, the optimal value of reel height also increased correspondingly, which had a significant interaction between reel speed and reel height. Figure 16c shows the influence of factors such as forward speed X_2 and reel height X_3 on the feeding success rate of reel Y_1. From the contour map, it could be seen that when reel speed was 3 rad/s, forward speed was 3.0-3.8 m/s and reel height was 500-550 mm, which response value was better, which had an implicit interaction between forward speed and reel height.

To get better operating parameters for the plant-correcting device, the optimization module of the Design-Expert data analysis software was used to optimize the solution. Set constraints: max Y_1, 2.5 rad/s$\leq x_1 \leq$3.0 rad/s, 0.3 m/s$\leq x_2 \leq$0.6 m/s, 500 mm$\leq x_3 \leq$600 mm. The optimized parameter combination was: reel speed, forward speed and reel height were 2.96 rad/s, 3.48 m/s and 541.67 mm respectively and the model predicted that the feeding success rate was 98.59%.

To ensure the accuracy of the optimization test, considering the operability of the actual test, the parameters such as reel speed, forward speed and reel height were corrected to 3 rad/s, 3.5 m/s and 540 mm. The test results showed that the feeding success rate was 98.73%, which was 0.14 percentage points higher than the theoretical model. The test and optimization results were essentially consistent, meeting the operational requirements of achieving a high feeding success rate and a low loss rate for garlic harvest.

4 Conclusions

1) To solve the problem of lodging garlic plants for harvest, a plant-correcting device was designed. Through regular rotation of the reel, the flexible rubber bars and plants bumped and deformed many times, lodging garlic plants were pulling and lifting to the conveyor, which improved the feeding success rate and reduced.

2) The contact deformation model and system energy equation were established in the contact process. Besides, in the stirring process, the plant-correcting conditions were established through dynamic simulation analysis of stem trajectories and the deflection model of stem was constructed. Furthermore, in the release process, the expression of bar rotation and plant offset bending curvature was constructed and the optimal number and distribution form of bars were determined. Meanwhile, the mechanism and key operating parameters of the auxiliary lifting mechanism of the divider were established and the transmission scheme of the plant-correcting device was defined.

3) Through the single-factor test, the influence of reel speed, forward speed, and reel height on the success feeding rate was analyzed under different bars distribution forms; Through multi-factor experiments, the interaction contour map of various factors was constructed and the influence degree on the evaluation index of feeding success rate was: reel speed>forward speed>reel height.

4) The prediction model of feeding success rate was established and the optimal parameter combination was obtained. When reel speed, forward speed, and reel height were 3 rad/s, 3.5 m/s, and 540 mm, the feeding success rate was 98.73%. The optimization factors were tested and verified, which met the operational requirements of a high feeding success rate and low loss rate of garlic harvest.

Acknowledgements

This research work was supported by China Agriculture Research System of MOF and MARA (CARS-24-D-01), the National Key R&D Program of China (Grant No. 2023YFD2001 200), and Shandong Province focuses on supporting the introduction of urgently needed and scarce talent projects in the region.

[References]

[1] Ekşi G, Gençler Özkan A M, Koyuncu M. Garlic and onions: An eastern tale. Journal of Ethnopharmacology, 2020; 253: 112675.
[2] Geng A J, Li X Y, Hou J L, Zhang J, Zhang Z L, Chong J. Design and experiment of automatic garlic seed directing device. Int J Agric & Biol Eng, 2020; 13(6): 85–93.
[3] Food and agriculture organization of the United Nations. Statistical database. http://faostat3.fao.org. Accessed on [2020-12-20].
[4] Food and Agriculture Organization of the United Nations. Garlic: Post-harvest operations. http://www.fao.org/fileadmin/user_upload/inpho/docs/Post_Harvest_Compendium_-_Garlic.pdf. 2007.
[5] Gardiner B, Berry P, Moulia B. Review: Wind impacts on plant growth, mechanics and damage. Plant Science, 2016; 245: 94–118
[6] Li C. Design and test of walking garlic combine harvester. Tai'an: Shandong Agricultural University, 2022; 103p. (in Chinese)
[7] Hou J L, Chen Y Y, Li T H, Wang L Y, Zhou J F. Development and test of 4s-6 garlic combine harvester. Journal of Engineering Science and Technology Review, 2020; 13(3): 106–114.
[8] Hou J L, Li C, Zhang Z L, Li T H, Li Y H, Wu Y Q. Design and test of double-row walking garlic combine harvester. Transactions of the CSAE, 2021; 36(12): 1–11.
[9] Wu W, Shah F, Ma B L. Understanding of crop lodging and agronomic strategies to improve the resilience of rapeseed production to climate change. Crop and Environment, 2022; 133-144.
[10] Qing Y R, Li Y M, Yang Y, Xu L, Ma Z. Development and experiments on reel with improved tine trajectory for harvesting oilseed rape. Biosystems Engineering, 2021; 206: 19–31.
[11] Hirai Y, Inoue E, Mori K. Investigation of Mechanical Interaction between a Combine Harvester Reel and Crop Stalks. Biosystems Engineering, 2002; 83(3): 307–317.
[12] Yu Z Y, Hu Z C, Peng B L, Gu F W, Yang L, Yang M J. Experimental determination of restitution coefficient of garlic bulb based on high-speed photography. Int J Agric & Biol Eng, 2021; 14(2): 81–90.
[13] Yang K, Hu Z C, Yu Z Y, Peng B L, Zhang Y H, Gu F W. Design and experiment of garlic harvesting and root cutting device based on deep learning target determination. Transactions of the CSAM, 2022; 53(1): 123–132. (in Chinese)
[14] Zhao D, Cai D M, Qin L X, Gao X, Huang W T, Liu C. Design and experiment of modularized garlic combine harvester. Transactions of the CSAM, 2020; 51(4): 95–102. (in Chinese)
[15] Sikandar H, Ammar A, Husain A, Kashif H, Muhammad A K, Tian R. Garlic, from medicinal herb to possible plant bioprotectant: A review. Scientia Horticulturae, 2022; 304: 111296.
[16] Tang Z, Liang Y Q, Zhang B, Wang M L, Zhang H, Li Y M. Effects of multi-sequence combination forces on creep characteristics of bales during wheat harvesting. Int J Agric & Biol Eng, 2021; 14(5): 88–99
[17] Xiao J Q, Ma R J, Chen Y. Effects of test levels on creep and relaxation characteristics parameters of stem for rice seedling grown in plastic cell tray. Int J Agric & Biol Eng, 2020; 13(4): 19–28
[18] Chen Y Q, Wang G P, Wang J T, Zhang P, Wang B, Hu Z C. Adaptabilities of different harvesters to peanut plants after cutting stalks. Int J Agric & Biol Eng, 2022; 15(2): 93–101.
[19] Qian Z J, Jin C Q, Zhang D G. Multiple frictional impact dynamics of threshing process between flexible tooth and grain kernel. Computers and Electronics in Agriculture, 2017; 141: 276–285.
[20] Kuwabara G, Kono K. Restitution coefficient in a collision between two spheres. Japanese Journal of Applied Physics, 1987; 26(8): 1230–1233.
[21] Lai C C, Huang A N, Chen C Y, Hsu W Y, Seville J P K, Kuo H P. Modification of the spherical particle spring-damping contact model from contact velocity dependent restitution coefficients. Powder Technology, 2022; 401: 117294.
[22] Bai J, Ma S C, Wang F L, Xing H N, Ma J Z, Wang M L. Performance of crop dividers with reference to harvesting lodged sugarcane. Sugar Tech, 2020; 22(5): 812–819.
[23] Jin C Q, Qi Y D, Liu G W, Yang T X, Ni Y L. Mechanism analysis and parameter optimization of soybean combine harvester reel. Transactions of the CSAM, 2023; 54(6): 104–113. (in Chinese)
[24] Hirai Y, Inoue E, Mori K. Application of a quasi-static stalk bending analysis to the dynamic response of rice and wheat stalks aligned by a combine harvester reel. Biosystems Engineering, 2004; 88(3): 281–294.
[25] Oduori M F, Mbuya T O, Sakai J, Inoue E. Modeling of crop stem deflection in the context of combine harvester reel design and operation. Agric Eng Int:CIGR Journal, 2012; 14(2): 8.
[26] Golpira H, Rovira-Más F, Golpira H, Saiz-Rubio V. Mathematical model-based redesign of chickpea harvester reel. Spanish Journal of Agricultural Research, 2021; 19(1): e0203.
[27] Tang Z, Zhang H T, Li H C, Li Y M, Ding Z, Chen J S. Developments of crawler steering gearbox for combine harvester straight forward and steering in situ. Int J Agric & Biol Eng, 2020; 13(1): 120–126.
[28] Wang G M, Song Y, Wang J B, Xiao M H, Cao Y L, Chen W Q, et al. Shift quality of tractors fitted with hydrostatic power split CVT during starting. Biosystems Engineering, 2020; 196: 183–201.
[29] Barr J, Desbiolles J, Ucgul M, Fielke J M. Bentleg furrow opener performance analysis using the discrete element method. Biosystems Engineering, 2020; 189: 99–115.
[30] Chandio F A, Li Y M, Xu L Z, Ma Z, Ahmad F, Cuong D M. Predicting 3D forces of disc tool and soil disturbance area using fuzzy logic model under sensor based soil-bin. Int J Agric & Biol Eng, 2020; 13(4): 77–84.
[31] Huang J C, Shen C, Ji A M, Tian K P, Zhang B, Li X W, et al. Design and test of two-wheeled walking hemp harvester. Int J Agric & Biol Eng, 2020; 13(1): 127–137.
[32] Gao X M, Xie H X, Gu F W, Wei H, Liu M J, Yan J C, et al. Optimization and experiment of key components in pneumatic peanut pod conveyor. Int J Agric & Biol Eng, 2020; 13(3): 100–107.
[33] Ji J T, Cheng Q, Jin X, Zhang Z H, Xie X L, Li M Y. Design and test of 2ZLX-2 transplanting machine for oil peony. Int J Agric & Biol Eng, 2020; 13(4): 61–69.